Cell

Multilevel Modulation of a Sensory Motor Circuit during *C. elegans* Sleep and Arousal

Julie Y. Cho[1,2] and Paul W. Sternberg[1,2,*]
[1]Division of Biology and Biological Engineering
[2]Howard Hughes Medical Institute
California Institute of Technology, Pasadena, CA 91125, USA
*Correspondence: pws@caltech.edu
http://dx.doi.org/10.1016/j.cell.2013.11.036

SUMMARY

Sleep is characterized by behavioral quiescence, homeostasis, increased arousal threshold, and rapid reversibility. Understanding how these properties are encoded by a neuronal circuit has been difficult, and no single molecular or neuronal pathway has been shown to be responsible for the regulation of sleep. Taking advantage of the well-mapped neuronal connections of *Caenorhabditis elegans* and the sleep-like states in this animal, we demonstrate the changed properties of both sensory neurons and downstream interneurons that mediate sleep and arousal. The ASH sensory neuron displays reduced sensitivity to stimuli in the sleep-like state, and the activity of the corresponding interneurons in ASH's motor circuit becomes asynchronous. Restoration of interneuron synchrony is sufficient for arousal. The multilevel circuit depression revealed provides an elegant strategy to promote a robust decrease in arousal while allowing for rapid reversibility of the sleep state.

INTRODUCTION

Sleep behavior is conserved and present in essentially all animal species as a lack of reactivity to sensory inputs, low activity, decreased conscious awareness, and rapid reversibility to wakefulness (Allada and Siegel, 2008; Siegel, 2001). Despite long-standing knowledge and characterization of these states, translation to a physiological or circuit definition has been difficult for many reasons. No single molecular or neuronal pathway has been shown to be responsible for the regulation of sleep, and incomplete knowledge of connections in sensory motor circuits of many studied species precludes interrogation of the flow of information that promotes sensory responses. Furthermore, the complexity and redundancy of the mammalian nervous system complicate the understanding of the flow of information. Here we use the nematode *C. elegans* to define sleep behavior in a simple sensory motor circuit.

C. elegans exhibits sleep-like behaviors during lethargus, a quiescent state during which locomotion and feeding are suppressed (Van Buskirk and Sternberg, 2007) and sensory arousal is decreased (Raizen et al., 2008). Lethargus lasts 2–3 hr, and like sleep, it exhibits homeostasis: upon disruption or deprivation during the normal resting period, there is a period of anachronistic rebound rest (Raizen et al., 2008). During lethargus, worms exhibit delayed or decreased avoidance behavior in response to both mechanical and chemical stimuli, and this response delay is reversible upon previous stimulation of the same neuron (Raizen et al., 2008). Quiescence as measured by decreased feeding and locomotory behavior is also present in adult satiety behavior (You et al., 2008). However, the dynamics of this state were not previously studied.

Lethargus invariably occurs during development after each of the four larval stages, and the timing of lethargus corresponds to increased expression of LIN-42, homolog of circadian regulator PER (Monsalve et al., 2011). In addition, several additional conserved regulators have been identified. Anachronistic quiescence is also induced by expression of epidermal growth factor (EGF) (Van Buskirk and Sternberg, 2007), a function conserved in mammals (Zimmerman et al., 2008) and *Drosophila* (Foltenyi et al., 2007), and sensory arousal can be depressed by PKG (Raizen et al., 2008), another well-conserved signaling protein. Conservation of sleep characteristics and molecular signaling suggests that the lethargus state in *C. elegans* could prove insightful in understanding sleep regulation.

The connections of the *C. elegans* nervous system are mapped (Ward et al., 1975; White et al., 1986), and functional circuits mediating avoidance defined (Bargmann, 2006). Avoidance behaviors are mediated by mechanosensory and chemosensory neurons that activate downstream circuit components to coordinate motor neuron activity and locomotion. The ASH sensory neuron drives an avoidance circuit and promotes immediate locomotory reversal (Figure 1A). When animals are presented with ASH-specific stimuli, ASH stimulates interneurons AVA and AVD, which in turn induces backward locomotion through stimulation of excitatory cholinergic motor neurons in the ventral cord (Figure 1A) (Guo et al., 2009; Hilliard et al., 2002, 2005). Evidence of altered arousal as measured by response delay to ASH-specific stimuli suggests modulation in the avoidance circuit during sleep behavior.

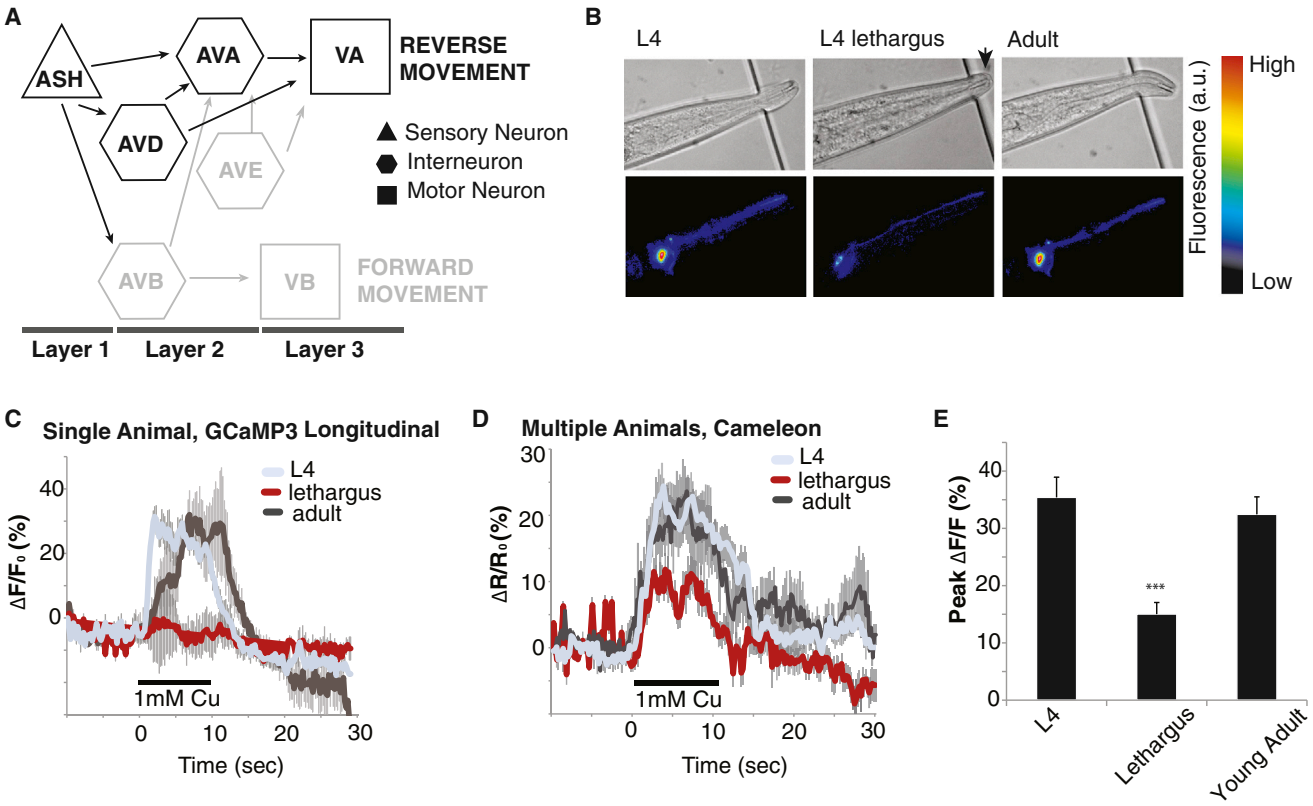

Figure 1. Sensory Depression Occurs in the ASH Polymodal Sensory Neuron

(A) Functional model of the avoidance circuit. The two polymodal ASH sensory neurons work through the two AVA and two AVD interneurons to promote reversal through the VA motorneurons. Neurons tested in the study are darkened.

(B) Single frames of GCaMP3 DIC and fluorescence recording in ASH over the L4, lethargus, and young adult stages. Arrow denotes the cuticle cap that marks lethargus.

(C) Representative GCaMP3 traces of a single worm as it transitions from L4 to lethargus to young adult.

(D) Average change in cameleon fluorescence in the ASH sensory neuron over time in a short calcium-imaging assay. L4 and lethargus response to 1 mM Cu^{2+} are shown (L4, n = 10; L4 lethargus, n = 11).

(E) The calcium increase in response to 1 mM Cu^{2+} is significantly decreased in lethargus (n = 11) as compared to L4 (n = 10) and young adult (n = 5; ***$p < 0.001$, Student's t test of equal variance). Error bars represent SEM.

See also Figure S1.

Many tools exist to probe and study neural circuits in *C. elegans*. Use of known transcriptional control regions of characterized genes drives expression of genetically encoded calcium sensors and allows measurement of activity in single or multiple cells. Cameleon is a dual-channel ratiometric reporter that corrects for changes in reporter expression over states, stages, and time. However, cameleon has slower dynamics because it involves energy exchange between two fluorophores, and GCaMP, a single-channel reporter, has better dynamic range. Therefore, we used both reporters: cameleon controlled for state-related changes in reporter expression, and GCaMP allowed measurement of smaller calcium events. Activity patterns observed can be mimicked using light-driven cation channels such as channelrhodopsin2 (ChR2). Similar to calcium sensors, ChR2 is genetically encoded and can be expressed in select cells using specific promoters as well as combinatorial approaches. These approaches can limit expression to either only cells where two promoters overlap or those that are unique to one promoter in the pair. These strategies allow measurement and activation of specific components of pertinent circuits. Here we use genetically encoded calcium sensors and light-driven channels to investigate the ASH circuit during sleep and waking. We find that multiple steps in the circuit are dampened during sleep.

RESULTS

ASH Sensory Neuron Exhibits Decreased Sensory Response to Disparate Stimuli in Lethargus

The amphid sensory neuron, ASH, senses multiple aversive stimuli including mechanical stimulation at the tip of the head and noxious chemical cues, such as copper, 1-octanol, or high osmolarity (Hilliard et al., 2005). We used a chemical stimulus to characterize ASH activity during a "sleep cycle" because it is more consistent and controllable than mechanical stimuli. We fabricated a modified version of a microfluidic olfactory

chip (Chronis et al., 2007) to accommodate and immobilize fourth larval stage (L4), lethargus, and young adult animals (Figure 1B). These devices permitted temporally controlled delivery of chemical stimuli and simultaneous fluorescence imaging from the ASH. Individual animals were assayed for a 6 hr period during which they were subjected to a brief stimulus every 30 min. ASH response was measured during these intervals using the calcium indicator GCaMP3 (Yizhar et al., 2011). Each animal was imaged before, during, and after lethargus. Chemosensory neurons use ligand-binding receptors to open ion channels (Bargmann, 2006), and ASH responds to the addition of 1 mM Cu^{2+} with a robust increase of calcium concentration in the L4 stage. During lethargus, the magnitude of ASH response to copper or glycerol decreases significantly, but full responsivity is recovered upon exit from lethargus (Figure 1C and Figure S1A available online).

To confirm this result and control for confounding factors such as changes in GCaMP expression and baseline calcium levels, short assays were performed using ratiometric imaging with the calcium sensor cameleon (Yizhar et al., 2011). In these assays, animals of each stage were loaded into the device, imaged within an hour of loading for both baseline and stimulus measurements, and discarded. These short assays were consistent with the longitudinal analysis: there was significant decrease in calcium levels as measured by the peak fluorescence change in response to the chemical copper and glycerol (Figures 1D, 1E, and S1A). Moreover, the availability of fluorescent indicator and baseline calcium concentration did not change sufficiently among behavioral states to account for the decrease in calcium levels (Figures S1B and S1C). Therefore, the calcium imaging data suggest that there are fewer calcium channels open, and thus the same stimulus is less able to excite the ASH sensory neuron during lethargus. This result is consistent with decreased calcium dynamics observed in the mechanosensory neuron ALM during lethargus (Schwarz et al., 2011). Furthermore, stimulus-evoked calcium transients were not ligand specific as evidenced by decreased response to both copper and glycerol and suggest that modulation in lethargus may affect general excitability or synaptic activity of the ASH neuron.

Basal Activity of AVA Is Reduced in Lethargus

We next examined the interneuron level in the circuit. Calcium levels in AVA oscillate, and increasing levels correspond to behavioral reversals (Ben Arous et al., 2010). We observed that oscillation of AVA activity is not regular and disappears in lethargus but reappears in the young adult animals (Figures S2A and S2B). Thus, we confirmed the published GCaMP3 findings in AVA with cameleon measurements. Furthermore, the basal activity and the context in which AVA receives input from ASH change during lethargus.

Synchrony between AVD and AVA Interneurons Is Lost in Lethargus

To assess activity across the top two layers of the circuit, we used animals expressing GCaMP3 in ASH, AVD, and AVA. To examine stimulus-driven interneuron activity, we measured response to an ASH-specific cue (1 M glycerol) (Hilliard et al., 2002), which has less variable dynamics (Figure S1A). Each 60 s trial consisted of a 10 s pulse of control buffer or glycerol; trials with discernable ASH responses were chosen, and instantaneous slopes were calculated over the imaging interval to represent the magnitude of the calcium increases. In young adult animals without stimulation, the timing of the calcium increases showed no association with the pulse of control buffer and did not occur during the stimulus interval (Figure S3D). However, after a glycerol stimulus, the increase of calcium in the AVD and AVA was associated with the stimulation interval (Figures 2B and 2C). AVD and AVA showed both decreased responsivity during lethargus as well as a loss of coordinated calcium activity. Animals in lethargus exhibited very little activity in the AVD and AVA, and fluctuating calcium levels during the glycerol stimulus were not significantly different from the period preceding the stimulus (Figure 2B). Because the magnitude of activity is considerably smaller in lethargus compared to the young adult, we had to normalize these measurements as binary values. Positive changes in fluorescence were thus counted as individual calcium increases. There were significantly more increases during the glycerol stimulus in the young adult, but often little activity was seen in AVA during lethargus even when AVD activity was noted (Figures 2C and 2E).

To test for association of ASH-interneuron and AVD-AVA activity, we compared the timing of initiation and duration of the calcium transients between neuron pairs by performing cross-correlation analysis between each of the neurons imaged. Comparing data for timing of calcium events between pairs allows us to assess functional correlation between neurons. This cross-correlation analysis indicates that when compared to the input ASH neuron, AVD transients exhibit a lag during lethargus, whereas AVA transients do not (Figures 2D and 2E). This observation suggests that when awake, AVD and AVA receive signal from the ASH and exhibit simultaneous calcium transients, whereas AVD in a lethargus animal is desynchronized with AVA. We further analyzed AVD and AVA for instances of repetitive calcium transients. There was a significant decrease of coupled trains during lethargus: a majority of the traces did not show activity in both neurons, and uncoupled activity was present during lethargus (Figures 2F and 2G). Moreover, the number of AVA-only traces did not differ significantly from the number of AVD-only traces (Figure 2G), suggesting that alterations of synaptic transmission are not specific to a particular synapse.

These results indicate that coupled activity in the command interneurons occurs in the awake state and not only may explain processing delay during lethargus but also suggests that synaptic transmission downstream of ASH becomes variable and differs across independent synapses. The altered efficacy of ASH-AVD and ASH-AVA synapses could be due to decreases in either presynaptic transmission or postsynaptic excitability. However, although it is possible that the ASH compartment presynaptic to AVD may vary independently from that which is presynaptic to AVA, the calcium measurements in the ASH show no indications that this is the case. In addition, synapse-specific changes or lags in activity usually show a general preference for a specific synapse rather than random or equal distribution as indicated by our AVD and AVA measurements (Figure 2G). The simplest interpretation is that there are postsynaptic changes in the downstream neurons.

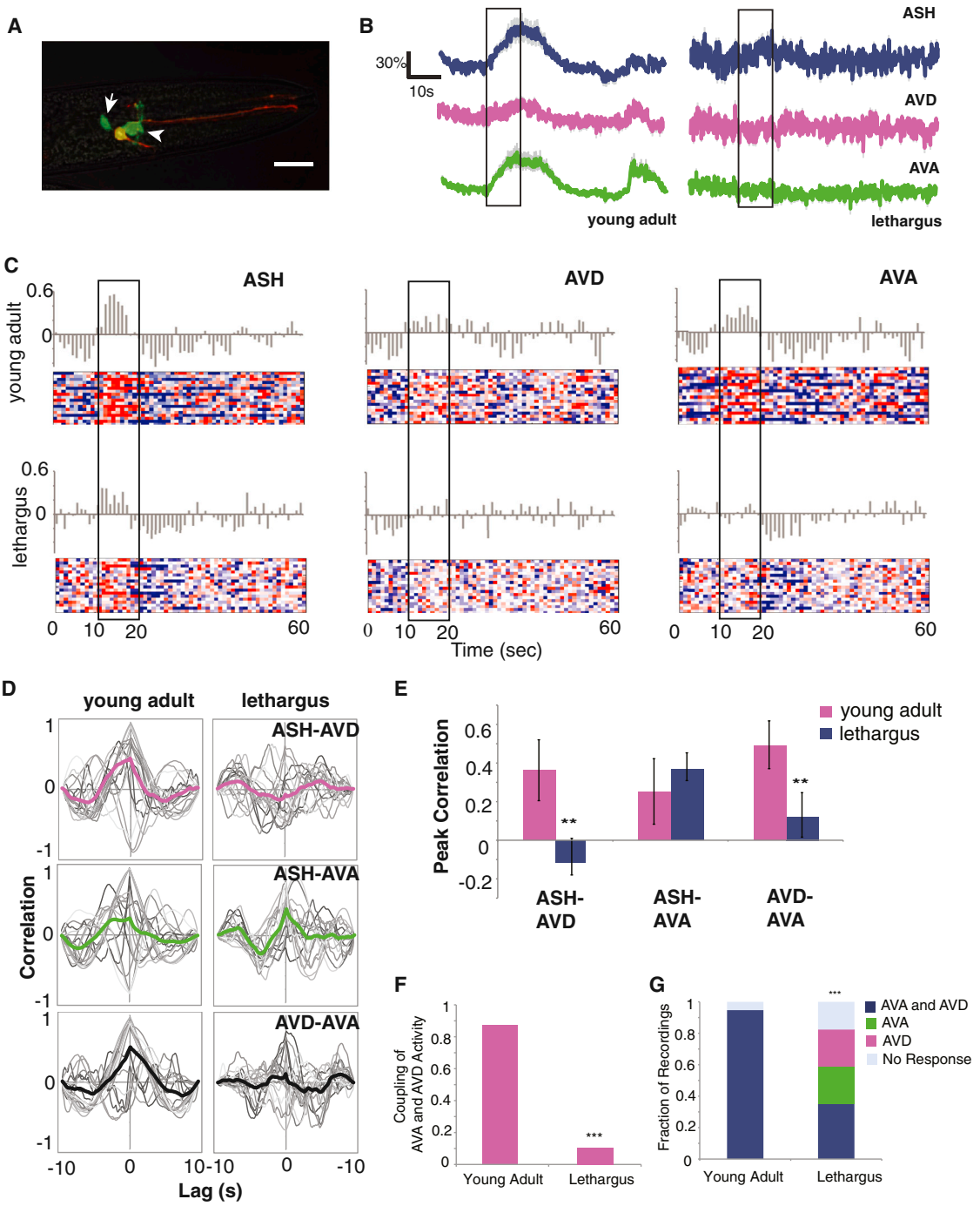

Figure 2. AVD Loses Synchrony with AVA in Lethargus

(A) Image of the neurons in which GCaMP3 was measured. ASH is marked by the presence of both GCaMP3 and mCherry, AVD is posterior (white arrow), and AVA is anterior (white arrowhead).

(B) Representative traces of a glycerol trial in a single animal in both lethargus and young adult. Scale bar represents 20 μm.

(C) Heatmap of 60 s trials denoting increase (red) and decrease (blue) in young adult (n = 18) and lethargus (n = 18). The proportions of increase or decrease were averaged across trials in 1 s bins and are denoted by the gray bars above the heatmaps.

(D) Cross-correlation of the stimulus interval between ASH-AVD, ASH-AVA, and AVA-AVD. Individual cross-correlations are shown as gray lines, the averages as the colored lines. Correlation of 1 is a perfect match, and correlation of −1 denotes an inverse relationship. AVD exhibits an average lag in response and shows a decreasing correlation with AVA during lethargus.

(E) Peak correlation values extracted from the cross-correlation analysis. AVD loses its synchronicity with ASH and AVD only in lethargus (n = 18; $p < 0.01$, Student's t test of unequal variance). AVA shows no decrease in correlation with ASH.

(legend continued on next page)

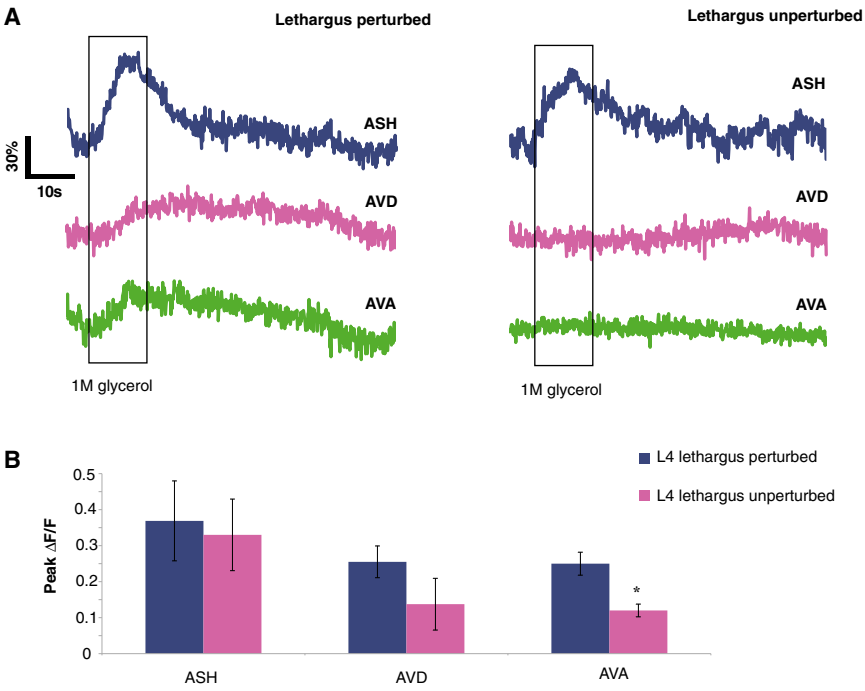

Figure 3. Loss of Synchrony Is Reversible and Can Be Separated from Magnitude of Calcium Increase in the ASH

(A) Representative GCaMP3 measurements of ASH, AVD, and AVA of a single worm in response to 1 M glycerol with and without previous mechanical stimulation during lethargus.

(B) Perturbation does not significantly affect peak increase in ASH as measured by GCaMP3, but it does cause significant increase in responsivity at the AVA (n = 4; *p < 0.01, Student's t test of unequal variance). Error bars represent SEM. See also Figure S3.

Loss of Synchrony Is Reversible and Can Be Separated from Magnitude of Calcium Increase in the ASH

Delayed response could also be a way for the circuit to function in all states (both awake and lethargus) when calcium activity in the ASH in decreased. In fact, decreased avoidance response to ASH-specific stimuli has been attributed to decreasing calcium activity in dopamine-treated animals (Ezcurra et al., 2011). Although neuromodulator-mediated sensory dampening is seen as decreases in behavioral response in the presence of serotonin or dopamine (Ezcurra et al., 2011), reversibility in behavior is more specific to the sleep state.

Furthermore, the source of reversibility is unknown. To analyze the cause of dynamics of reversibility, we need to know whether it is the magnitude of calcium increase at a sensory neuron or the response of downstream components that is reversible.

Therefore, we measured lethargus animals expressing GCaMP in ASH, AVD, and AVA in the microfluidic chip with and without a mechanical stimuli preceding glycerol stimulation. Individual animals showed the same trend: calcium increase in the ASH did not differ significantly between unperturbed and perturbed trials (Figures 3A and 3B), but the activity in the downstream interneurons was both coordinated and immediate in trials following mechanical stimulation (Figure 3A). This result indicates that although varying presynaptic input from the ASH may change circuit function and behavior, there are other postsynaptic factors that modulate transmission at these synapses. Furthermore, these changes are dependent upon previous stimulation at the level of the interneurons.

Modulation in Lethargus also Lies downstream of ASH Depolarization

We validated imaging data and assessed the contribution of downstream neurons to lethargus behavior using the genetically encoded light-activated cation channel ChR2. In the presence of its cofactor, all-trans retinal (ATR), ChR2 allows control of both the extent and timing of cellular depolarization through optical stimulation (Lindsay et al., 2011; Narayan et al., 2011; Zhang et al., 2007). Changes in the sensory response to ASH-mediated noxious stimuli (such as copper or glycerol) are modulated by the presence of food or exogenous application of dopamine, but these responses are modality specific and are absent in response to mechanical stimuli (Ezcurra et al., 2011). Optogenetic activation of ASH was shown to be unaffected by changing conditions (Ezcurra et al., 2011). Direct control of ion channels and normalization of the initial current injection allow for better assessment of the downstream components of the avoidance circuit by bypassing ligand binding and associated membrane depolarization in ASH.

Neuron classes in each level of the avoidance circuit were individually depolarized. We used animals in which ChR2 is expressed exclusively in the ASH (Ezcurra et al., 2011) and found that light-driven activation induced robust and active reversal behavior in both the L4 and young adult animals (Figure 4B). However, behavioral response delay persists upon ChR2-mediated ASH depolarization during lethargus: the average time to respond to the ChR2 stimulation increased from 2 s to 18 s in lethargus (Figure 4B). Therefore, behavioral delay is not likely due to the decrease in receptor-associated depolarization at the ASH, is different from dopamine-mediated modulation, and suggests the existence of additional modulation in downstream components of the circuit. This conclusion is further supported by our finding that regional stimulation of ChR2 in the ASH dendrite using targeted illumination can in fact induce calcium increase as measured by GCaMP3 in and out of lethargus (Figure S3E).

(F) Quantification of trials in which GCaMP3 measurements of AVA and AVD showed corresponding trains of calcium increase during the course of the trial. The majority of trials in the young adult (0.86, n = 23) showed coupled activity, but this coupling decreased significantly in lethargus ($p < 0.000001$, 0.12, n = 16).

(G) Many of the trials in lethargus showed activity in either AVA or AVD, whereas young adult animals did not show any instances of this pattern of activity ($p < 0.0001$). Error bars represent SEM. See also Figure S2.

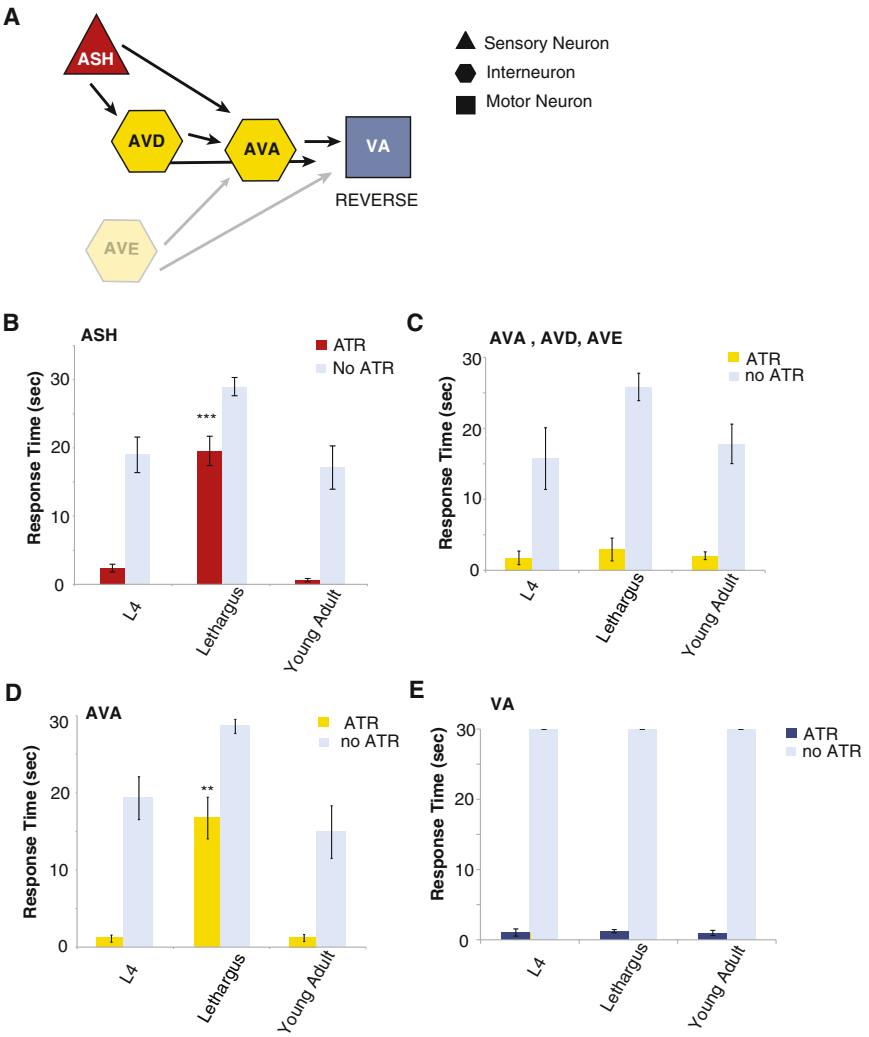

Figure 4. Sensory Modulation Occurs downstream of ASH Depolarization

(A) Schematic diagram of the neurons manipulated to generate reversal. ASH promotes activity at the AVD and AVA interneurons.

(B) Behavioral response times to ASH depolarization using channelrhodopsin. The mean ± SEM values are shown: L4 (n = 13), lethargus (n = 9), adult (n = 7); ***p = 0.0001, ANOVA. All ATR-treated animals were compared to their paired non-ATR-treated controls: L4 (n = 13), lethargus (n = 9), adult (n = 7); $p < 0.0001$, Student's t test of unequal variance.

(C) AVA, AVE, and AVD were depolarized using channelrhodopsin. Avoidance behavior did not differ significantly between worms in and out of lethargus: L4 (n = 7), lethargus (n = 6), adult (n = 6), ANOVA. All ATR-treated animals were compared to their paired non-ATR-treated controls: L4 (n = 7), lethargus (n = 6), adult (n = 6); $p < 0.0001$, Student's t test of equal variance.

(D) Depolarization of AVA without the other command interneurons showed a significant delay in lethargus (n = 13) when compared with L4 (n = 7) and adult (n = 6); **$p < 0.001$, ANOVA. All ATR-treated animals were compared to their paired non-ATR-treated controls: L4 (n = 6), lethargus (n = 10), adult (n = 6); $p < 0.0001$, Student's t test of unequal variance.

(E) Depolarization of cholinergic motorneurons with channelrhodopsin. L4 (n = 5), lethargus (n = 5), adult (n = 5), ANOVA. All ATR-treated animals were compared to their paired non-ATR-treated controls: L4 (n = 13), lethargus (n = 9), adult (n = 7); ***$p < 0.0001$, Student's t test of equal variance. Error bars represent SEM. See also Figure S4 and Movies S1 and S2.

Activation of Multiple Command Interneurons Is Sufficient to Induce Awake-like Behavior

We next activated the downstream command interneurons using the *nmr-1* transcriptional control region to drive ChR2 in AVA, AVD, and AVE (Figure S4A). AVA activity promotes avoidance behavior (Chalfie et al., 1985), and upon direct depolarization of the reverse command interneurons, animals both in and out of lethargus responded immediately (Figure 4C). We further tested activation of AVA alone by targeted illumination of the AVA in animals expressing ChR2 in AVA and RIG. RIG is an interneuron that does not induce changes in locomotion upon activation by ChR2 (Schmitt et al., 2012). Activation of ChR2 in this line with whole-body or targeted illumination of AVA alone induces robust reversal in adult worms (Schmitt et al., 2012) but fails to do so consistently or quickly in lethargus (Figures 4D and S5E–S5G; Movies S1 and S2). We used a strain expressing ChR2 in AVA and RIG for AVA-targeted illumination experiments because the AVA is anatomically more distant from the RIG as compared to the command interneurons or the RIM. However, we also tested the AVA with RIM and found similar results to those seen in AVA and RIG (Figure S5F). Thus, if and when interneurons are activated together, a rapid behavioral response follows. The lack of a rapid response upon direct ASH depolarization indicates that transmission of excitatory information from the sensory to the interneurons is decreased or delayed in lethargus.

It is conceivable that that the inability of AVA activation to generate immediate reversal during lethargus may be due to decreasing ChR2 expression in AVA. Therefore, we measured the expression level of ChR2 in the AVA and found that it did not change significantly in and out of lethargus (Figures S4B and S4D). Lack of altered expression suggests that AVA alone is not sufficient to trigger robust reversals during lethargus. Multiple interneuron input is a crucial component for consistent generation of immediate reversals.

Direct activation of the cholinergic motor neurons including the VA reverse motor neurons showed no significant response latency between the responses of L4, lethargus, and young adulthood (Figure 4F), suggesting that the modulation of signaling during lethargus did not occur downstream of the AVA interneuron and remained consistent with previous data indicating that the amount of contraction did not change in lethargus (Dabbish and Raizen, 2011). The importance of synchronous activity

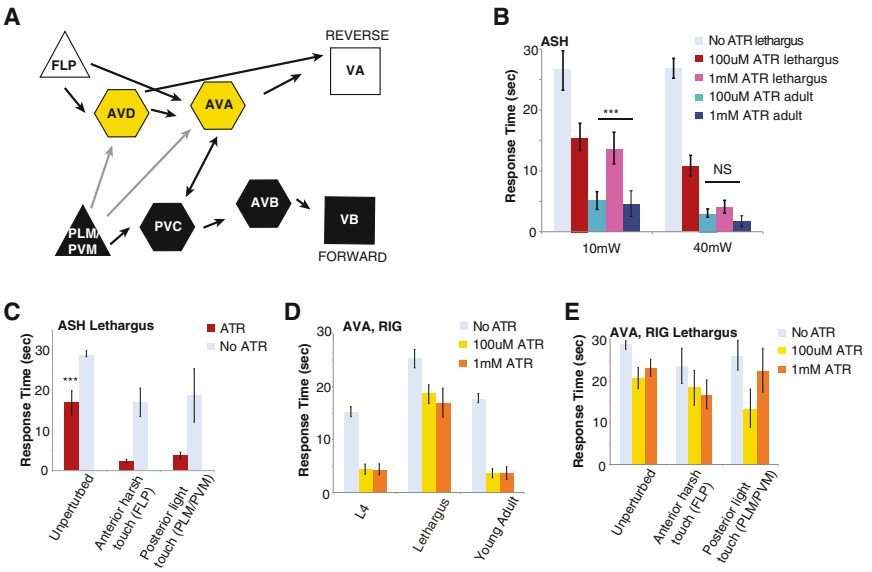

Figure 5. Reversibility Arises from Interneuron Activation but Requires Simultaneous Input to Both AVD and AVA

(A) Schematic diagram of the neurons manipulated to generate reverse locomotion. Multiple sensory cues and neurons, including ASH and FLP, can induce reversal (Chatzigeorgiou and Schafer, 2011; Hilliard et al., 2002). FLP neurons are activated in response to harsh mechanical stimulation at the body wall and act independently of ASH to promote activity at the AVD and AVA interneurons. The PLM and PVM mechanosensory neurons work through the PVC interneuron but are also synaptically connected with the AVA and AVD to generate forward locomotion in response to tail touch.

(B) Behavioral response to 10 mW and 40 mW of optical stimulation of ChR2 in lethargus and young adult animals at 100 μM and 1 mM ATR concentrations.

(C) ASH of lethargus animals were depolarized with ChR2 unperturbed (n = 21), after harsh touch at the body wall (n = 9), and after tail touch (n = 12). Both perturbations suppressed the delay in reversal; ***p < 0.0001, ANOVA. All ATR-treated animals were compared to their paired non-ATR-treated controls unperturbed (n = 21), after harsh touch at the body wall (n = 9), and after tail touch (n = 12); p < 0.0001, Student's t test of unequal variance.

(D) AVA of lethargus animals grown in 0, 100 μM, or 1 mM ATR were depolarized with ChR2 unpertubed (n = 23), after harsh touch (n = 10), and after tail touch (n = 13). No significant difference was seen between animals grown on 100 μM and 1 mM ATR. All ATR-treated animals were compared to their paired non-ATR-treated controls unperturbed (n = 23), after harsh touch at the body wall (n = 10), and after tail touch (n = 13); p < 0.0001, Student's t test of unequal variance.

(E) Even with increased ATR concentration at 1 mM, depolarization of AVA in animals continued to show a significant delay in lethargus (n = 11) when compared with that in L4 (n = 13) and adult (n = 9); ***p < 0.0001, ANOVA. No significant difference was seen between animals grown on 100 μM and 1 mM ATR.

Error bars represent SEM. See also Figure S5.

in multiple neurons reflects the signal amplification that occurs in the circuit to promote reversal. Amplification can occur through two not necessarily distinct mechanisms: excitation of multiple interneurons by ASH and further amplification of that signal by multiple feedforward loops in the circuit (Figure 4A).

Increasing the Extent of ASH but Not AVA Depolarization Can Elicit Immediate Response

Previously published work describes the avoidance circuit as a coherent type 1 feedforward loop, the dynamics of which have been modeled (Figure S5A) (Kashtan et al., 2004). This circuit motif creates delay by preventing processing in the AVA until both ASH and AVD are active (Kashtan et al., 2004). Our simulation of dynamics using the published model shows that adjusting the threshold or ratio of transfer at the ASH to interneuron synapses (even in the absence of input change) can cause a delay, which can be shortened by increasing activity at the ASH (Figure S5B). We therefore stimulated ChR2-expressing ASH neurons in a graded manner. To more strongly activate ASH, we used a 100-fold higher concentration of ATR and a 2.5-fold stronger light intensity. When subjected to this stronger stimulus, animals in lethargus displayed a reduced behavioral delay not significantly different from that of young adults (Figures 5C, S6A, and S6B). These results are consistent with the model and suggest that either the threshold or transfer at the synapse changes during lethargus, requiring significantly more presynaptic depolarization to elicit an immediate response. Increasing ASH input should increase activity at the AVD as well as the AVA, implying that the increased input to motor neurons may no longer be linear and is possibly exponential. Increased current injection at RIM and AVA does not suppress response delay (Figure 5E), raising the possibility that a single command interneuron may not be able to output sufficient signal to the motor neurons to generate immediate response and that synchronous activation of the command interneurons is likely necessary for rapid reversal.

Response Delay to ASH Depolarization Is Reversible upon Previous Stimulation

To further understand the decreased transmission between sensory and interneurons during lethargus, we stimulated interneurons through an ASH-independent circuit (Figure 5A). Mechanosensation at the body wall promotes reversal by activating the AVA and AVD command interneurons independent of ASH (Chatzigeorgiou and Schafer, 2011; Li et al., 2011). FLP, a mechanosensory neuron, responds to harsh touch to the anterior body (Chatzigeorgiou and Schafer, 2011). When animals are woken by a harsh touch, they reverse immediately. After a full reversal, animals are more responsive to ChR2 stimulation, and the average response delay to ChR2-induced ASH depolarization is 2 s, suppressing the response delay normally seen in lethargus (Figure 5B). Surprisingly, promoting forward locomotion with PLM/PVM-mediated tail touch, which functionally should inhibit AVD and AVA, also suppressed response delay (Figure 5B). It is thus not important whether the animals are moving forward or backward but that they are active. Waking the animal during lethargus does not suppress response delay to AVA depolarization (Figure 5D), indicating that input into multiple

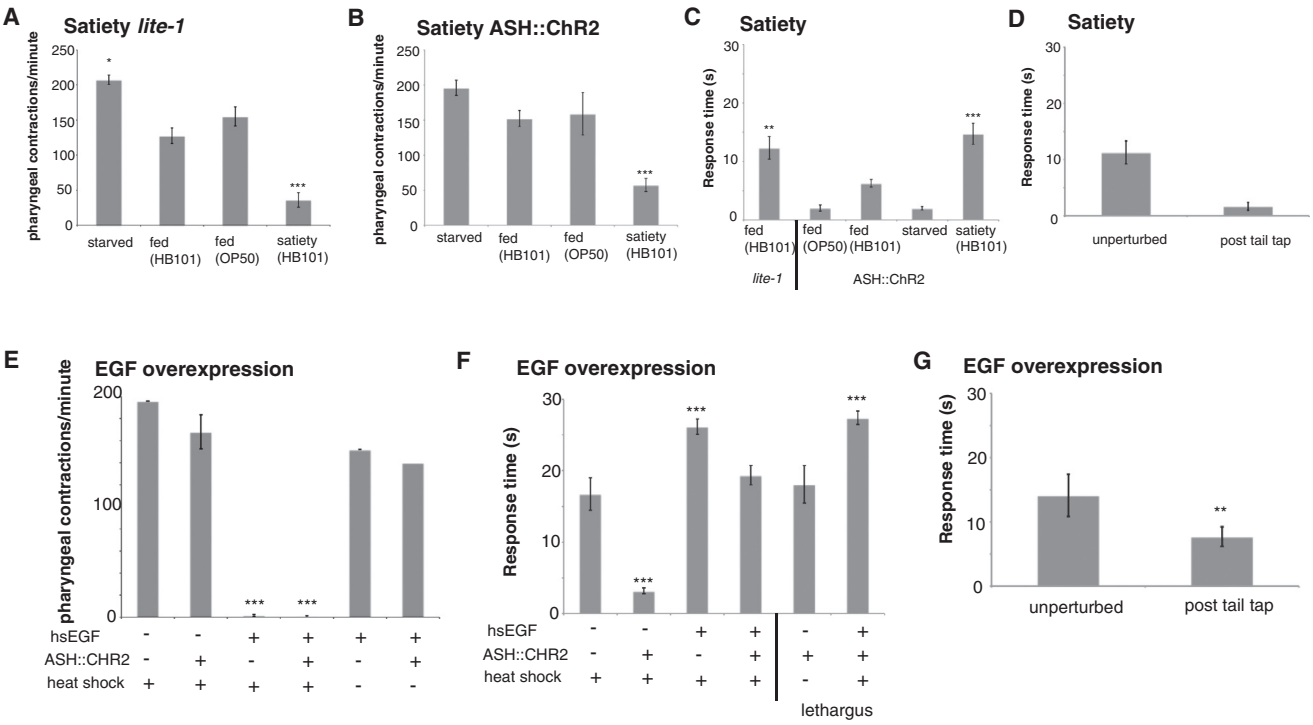

Figure 6. Circuit Modulations in Lethargus Are Dependent on Arousal State

(A) Feeding activity of *lite-1* animals (which have decreased response to blue light) as indicated by pharyngeal contractions in response to starvation (n = 8), feeding on OP-50 (n = 9), feeding on HB101 (n = 5), and feeding after 12 hr of starvation, i.e., satiety assay (n = 14). The mean ± SEM values are shown; *p = 0.01, ***p = 0.0001, ANOVA.

(B) Feeding activity of ASH::ChR2 animals as indicated by pharyngeal contractions in response to starvation (n = 8), feeding on OP-50 (n = 5), feeding on HB101 (n = 13), and feeding after 12 hr of starvation, i.e., satiety assay (n = 17). The mean ± SEM values are shown; ***p = 0.0001, ANOVA.

(C) Reversal following light activation of *lite-1* (n = 8), ASH::ChR2 animals that were subjected to starvation (n = 20), feeding on OP-50 (n = 13), feeding on HB101 (n = 8), and feeding after 12 hr of starvation, i.e., satiety assay (n = 17). The mean ± SEM values are shown; **p = 0.001, ***p = 0.0001, ANOVA.

(D) Reversal following light activation of ASH::ChR2 animals following the satiety assay before perturbation (n = 11) and after tail tap (n = 11); ***p = 0.0001, Student's t test of unequal variance.

(E) Feeding activity as indicated by pharyngeal contractions were measured to assess activity levels of the animals following EGF overexpression by heat shock. Only animals with the heat-shock EGF transgene (hsEGF) that were treated with heat shock showed decrease in activity. The mean ± SEM values are shown: heat shock *lite-1* (n = 5), heat shock ASH::ChR2 (n = 5), heat shock hsEGF (n = 11), heat shock hsEGF ASH::ChR2 (n = 7), hsEGF (n = 5), ASH::ChR2 (n = 5); ***p = 0.0001, ANOVA.

(F) Reversal following light activation of heat-shocked animals. The mean ± SEM values are shown: heat shock *lite-1* (n = 11), heat shock ASH::ChR2 (n = 17), heat shock hsEGF (n = 18), heat shock hsEGF ASH::ChR2 (n = 16), heat shock ASH::ChR2 in lethargus (n = 10), heat shock hsEGF ASH::ChR2 in lethargus (n = 9); ***p = 0.0001, ANOVA.

(G) Reversal following light activation of hsEGF ASH::ChR2 animals before perturbation (n = 11) and after tail tap (n = 11); ***p = 0.0001, Student's t test of unequal variance.

Error bars represent SEM. See also Figure S6.

command neurons is required. These results suggest that there is an awake state that determines the interneuron resistance to signal processing, and waking primes the interneurons to respond to sensory stimuli.

Circuit Modulations Seen in Lethargus Are General and Dependent on Arousal State

Behavioral quiescence can be observed outside of lethargus and in the adult stage during satiety behavior (You et al., 2008) and during EGF overexpression (Van Buskirk and Sternberg, 2007). Satiety can be induced with high-nutrient food and is enhanced when a long period of starvation is followed with food (You et al., 2008). We examined the behavior of animals 3 hr after refeeding and observed quiescence, as measured by pharyngeal pumping and locomotion (Figures 6A and 6B). Animals that were fasted and refed showed delayed response to ASH activation with ChR2 when compared with starved or continuously fed animals (Figure 6C). Moreover, this delay was reversible and was suppressed by previous mechanical stimulation (Figure 6D). These results show that sleep-like behavior is not restricted to lethargus and suggest that the changes in the avoidance circuit are not tied to the developmental stage but physiological state of the animal.

EGF overexpression in young adult animals showed similar results. EGF signaling was implicated as a quiescence-promoting component during lethargus, and anachronistic expression

strongly induces quiescence (Van Buskirk and Sternberg, 2007). Therefore, we induced quiescence by overexpressing EGF in young adult animals (Figure 6E) and found that animals had a delayed response to ASH activation comparable to lethargus (Figure 6F). Also, delayed response due to EGF could also be reversed upon previous stimulation by a tail tap (Figure 6G). These results show that sleep-like behavior induced outside of lethargus by satiety and one component of lethargus signaling is effective in replicating the behavioral dynamics.

In addition, we found that rebound homeostatic behavior seen following disruption of lethargus (Raizen et al., 2008) can be seen in response to ChR2 activation (Figure S6E). These data suggest that lethargus occurs by downstream circuit modulation and can be driven and adjusted by previous activity and by environmental factors. Furthermore, these observations eliminate the possibility of developmental factors being the primary driver of neuronal modulation.

We also tested whether the observed sensory neuron modulation is restricted to ASH or to circuits mediating avoidance. We chose to study the gustastatory neuron, ASE, during and out of lethargus. Unlike ASH, ASE senses attractive stimuli, like preferred salt concentration, has no mechanical component, and promotes forward locomotion. We found that ASE also shows decreased calcium transients during lethargus (Figure S6F), implying that circuit modulations are likely general across the sensory layer, and similar modulation likely exists in the forward command interneurons.

DISCUSSION

We examined the well-characterized ASH avoidance circuit during sleep and waking and found that decreased arousal during sleep stems from not only the worm's inability to robustly sense the incoming stimulus but also a failure to activate components of the circuit that promote avoidance in the awake state. We found significant modulation in both sensory and command interneuron activity during lethargus and confirmed the function of observed activity patterns using channelrhopdopsin to optically control activity in single or select groups of neurons. We also find that dampened sensory activity in the ASH neuron is likely correlated with the presence of sleep drivers, is constant during lethargus, and is minimally altered in response to optogenetic stimuli after mechanical stimulation preceding the measured trial duration. This neuronal activity is in stark contrast to the dynamics of behavior: sensory response to ASH activation by chemical stimuli is immediate upon previous waking with mechanical stimuli. However, changes in dynamics are well correlated with coordinated activity of the command interneurons AVD and AVA. Moreover, this coordinated activity that is lost during quiescence is recovered upon waking.

How might activation of interneurons by one sensory neuron sensitize them to other sensory neurons? One mechanism of decreasing threshold is to make the interneuron more receptive to presynaptic input by activity-driven changes in receptor localization (Metherate, 2004; Metherate and Hsieh, 2004). In addition, activity-driven changes in synaptic tranmission and transfer can be readily explained by disinhibition (Letzkus et al., 2011) or neurotransmitter availability. The fast dynamics of reversibility during sleep make it unlikely that neuromodulators are directly responsible for the reversibility because unbinding from targets and breakdown or sequestration of peptides would not be possible in the timescale of behavioral dynamics (milliseconds to seconds). In addition, the mediation of reversible transmission by a secondary intermediate outside of the sensory motor circuit is precluded by the lack of candidates with the proper connectivity to all sensory neurons or even the sensory neurons published or tested in this work (White et al., 1986).

Both decreased sensory transduction and reversible resistance in transmission of excitatory information downstream occur, and the presence of these modulations pose interesting questions about the utility of having multiple levels of modulation. Decreasing the magnitude of ASH response results in decreased signal processed downstream and, theoretically, in a smaller probability of reaching threshold to relay information to downstream components of the circuit (Figures S3B and S4A). This type of sensory gating would help prolong inactivity in the sensory motor circuit and promote behavioral quiescence. However, direct alteration of the response of individual sensory neurons after waking or even all sensory neurons after waking would perpetuate a long awake state because the nervous system would not be sufficiently gated and thus might continue responding to basal sensory stimuli as well as mechanical stimuli from locomotion. Thus, if sleep and wakefulness in the worm are regulated only by gating and lack of gating, respectively, at the sensory neuron, then the dynamics in the circuit create a positive feedback loop because activity in the circuit would sensitize the sensory neuron and promote more activity in the circuit, and so on. Furthermore, constant decrease in ASH activity makes the circuit more sensitive to small changes in signal transduction or synaptic transmission to AVA and AVD, lengthening the range of behavioral delay and decreasing the probability of downstream synchronization (Figures S3A and S3B). Dynamic sensitization of the command interneurons allows for increased probability of coordinated activity upon previous stimulation but requires sensory input to multiple command neurons (Figure 7). Therefore, the use of coordinated activity in downstream components offers flexibility and fast behavioral dynamics while simultaneously ensuring that waking leads to sensitivity to all modalities as well as sensory neurons that converge upon the command neurons.

We found that behavioral delay and reversibility are not exclusively limited to lethargus: they occur with EGF expression and with quiescence induced by satiety, indicating that these circuit modulations are due to behavioral state and not developmental stage. Thus, these results are more relevant to understanding behavioral states across species. Also, sensory dampening is likely general in sensory motor circuits, and sensory neurons associated with food and attractive stimuli are dampened in addition to those for pain and noxious stimuli.

Past circuit understanding of sleep is limited to a general understanding of loss of synchrony between cortex and thalamus due to inability of the thalamus to relay information to the cortex (Jones, 2009; Magnin et al., 2010). We have demonstrated similar changes of information relay from sensory to command interneurons in a simple circuit of *C. elegans*. Decrease in sensory signaling contributes to, but is not the sole factor of,

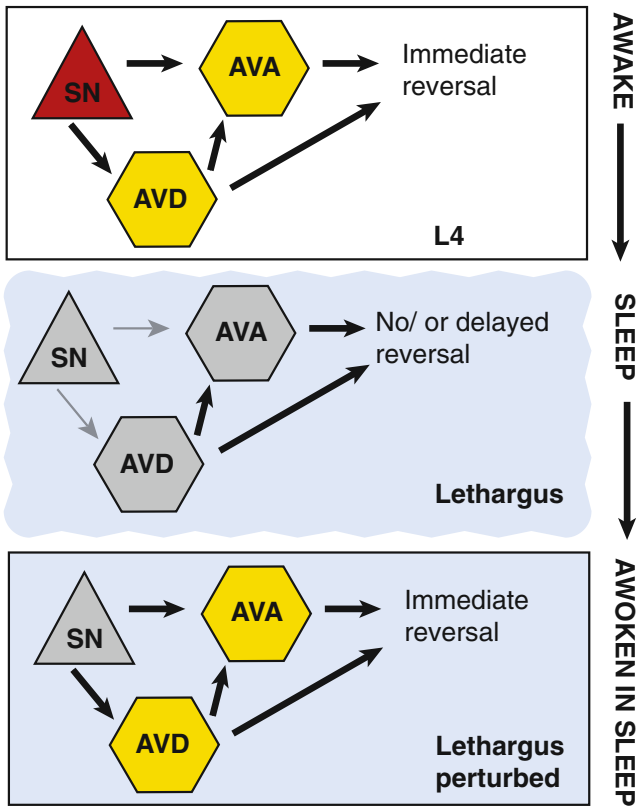

Figure 7. Waking Sensitizes the Interneurons for Coordinated Activity

Schematic model of activity in awake animals, during lethargus, and waking during lethargus. Grayed neurons indicate modulated function: activity of sensory neuron (SN) in lethargus indicates decreased excitability, and the variable timing and dampening of interneuron activity suggest decreased excitability of and/or synaptic transmission of interneurons (AVD and AVA). Arrows mark synaptic connections between the neurons, and the gray thin lines denote decrease in transmission across the sensory interneuron synapses during lethargus.

changing information relay. Excitability of the downstream command interneurons is also likely altered and serves as a point for reversible function of the circuit during the sleep-like state. Thus, small changes in dynamics at multiple levels promote and prolong quiescence while allowing reversibility of behavior upon sufficient stimulus by using circuit components that appear redundant but serve to amplify or suppress input signal. The *C. elegans* nervous system is condensed when compared to a mammalian nervous system. We can then conjecture that a sensory neuron in the worm may serve to perform both sensory functions and the processing that presumably occur downstream in other less compact neural circuits. Regardless, these components of multilevel modulation serve as one strategy for generating the dynamic behaviors seen in sleep.

EXPERIMENTAL PROCEDURES

Strains

Caenorhabditis elegans strains were maintained under standard conditions at 20°C (Brenner, 1974). The following strains were used in this study:

ASH ChR2: AQ2235 *lite-1(ce314)*; *ljIs114[Pgpa-13::FLPase; Psra-6::FTF::ChR2::YFP]* (Ezcurra et al., 2011);

AVA, RIM ChR2: ZX1038 *lin-15(n765ts); lite-1(ce314); zxEx704[pflp18::loxP::LacZ::STOP::loxP:: ChR2::mCherry::SL2::GFP* (80 ng/μl); *pgpa-14::Cre* (80 ng/μl); *lin-15+]*(Schmitt et al., 2012);

AVA, RIG ChR2: ZX1020 *lin-15(n765ts); zxEx717[pflp18::FRT::mCherry::STOP::FRT:: ChR2::YFP* (80 ng/μl); *prig-3::FLP* (80 ng/μl); *lin-15+]*(Schmitt et al., 2012);

Cholinergic motor neuron ChR2: EG5096 [*Punc-17:ChR2::mCherry*] (Dabbish and Raizen, 2011);

ASH ChR2 with ASH, AVD, and AVA GCaMP3: SRS85 *sraIs49 [nmr-1p::G-CaMP; unc-119(+)]; lite-1(ce314); sraEx80 [sra-6p::chop-2(H134R)::mCherry; osm-10p::G-CaMP; unc-122p::mCherry]* (Guo et al., 2009);

AVA cameleon: PS5955 (*Prig-3:: cameleon*);

ASH cameleon: *ljEx95[Psra-6::YC2.12]*(Hilliard et al., 2005).

Molecular Biology

The genetically encoded light-activated channelrhodopsin gene *ChR2* (a gift from the Deisseroth lab) was cloned into the pPD96.52 Fire vector (Addgene) to generate a *ChR2::YFP* fusion with the *unc-54 3′utr*. This construct was fused to a 5 kb sequence from upstream of the *nmr-1* gene previously demonstrated to drive expression in AVA and AVD. Expression was confirmed in AVA, AVD, and AVD interneurons (Guo et al., 2009).

Chip Fabrication

We designed chips in AutoCAD (Autodesk) and sent the design to a mask-making service (Photosciences), which provided the chrome masks. We created the master molds by spin casting at 3,000 rpm and patterning a 19 μm-thick layer of SU-8 photoresist (MicroChem) on bare silicon wafers. We used previously published procedures to prepare the master molds for use with polydimethylsiloxane (PDMS) and perform the soft lithography to make the PDMS replicas (Park et al., 2006). The PDMS replicas were treated with air plasma (40W for 12 s) to activate the PDMS surface and manually bond it to a coverslip. The chips were ethanol treated and flushed with FU-18 before use.

Calcium Imaging

Calcium imaging was performed in a microfluidic device essentially as described (Chronis et al., 2007). The device was altered in only the part of the chip that constrains the worm to fit different developmental stages. Several versions were made in which the dimensions were scaled to fit an animal 600 μm in length and 30–60 μm in diameter. The flow of stimuli and buffers in the device was controlled using an external valve system to regulate pressure at the various inlets, which modified the pattern of flow. External components were built according to published protocols to automate the valve system (Rafael Gómez-Sjöberg, Microfluidics Lab, Lawrence Berkeley National Laboratory), and valves were controlled using LabView software (National Instruments). Fluorescence time-lapse imaging (100 ms exposures, 5 Hz) was performed on a Zeiss Axioscope inverted microscope with a 40× air objective and an Andor EMCCD camera. Animals were presented with alternating streams of S-basal complete buffer and stimulant (Cu^{2+} or glycerol) in S-complete buffer. All image analysis was done using a custom script written in Matlab: after background subtraction, total fluorescence intensity was measured from the individual regions of interest (ROIs) corresponding to the cell body. No adjustments were done for photobleaching as there was minimal evidence of such with the low-intensity light exposure.

Analysis of Calcium Events

Exponential smoothing of the calcium imaging data was performed in Matlab (alpha value of 0.05), and instantaneous time derivatives were calculated for each time point. These values were plotted in a raster plot (Figures 2C and S3C) and were characterized as a calcium increase (>0) or decrease (<0). These events were further binned into 1 s bins to quantify the probability of these events during the duration of the imaging and response to buffer or glycerol. Cross-correlation was performed on the data of corresponding ASH-AVD, ASH-AVA, and AVD-AVA traces. The value at lag time = 0 or peak correlation was used to assess differences between different neuron sets and conditions.

Behavior

Unless otherwise stated, AQ2235 animals were grown in the dark with 10 μM ATR and were illuminated with blue light (425–475 nm) from an LED device (Phillips LumiLEDS) at 12 mW intensity at the level of the plate. EG5096 and ZX1020 animals were grown in the dark with 100 μM ATR, picked onto a new ATR plate, allowed to rest for 10 min, and illuminated with blue light (425–475 nm) from an LED device (Phillips LumiLEDS) at 12 mW and 30 mW intensity at the level of the plate. Animals were stimulated with an LED device when stationary or exhibiting forward locomotion and imaged during the assay for behavioral analysis with a Leica stereomicroscope and a Unibrain camera with Unibrain software. Reversal was scored as posteriorward movement that was greater than the length of the worm's head. Three trials were performed for each worm, and the interval between trials was 30 s.

Worms were perturbed for the waking assays by harsh touch with a worm pick immediately anterior to the middle of the worm (marked by the vulva) or by tail touch with an eyelash drawn across the tail of the worm. ChR2 assays were performed when the animals exhibited stationary behavior or forward locomotion (all stimulations were performed within 30 s of the perturbation).

Worms that were tested for lethargus homeostasis by 30 min perturbation in lethargus or L4 stage were stimulated by tail touch with an eyelash drawn across the tail of the worm every minute or when the worm was observed to be quiescent (whichever came first). ChR2 assays were performed when the animals exhibited stationary behavior for the baseline measurement. Then, animals were again perturbed with tail touch and tested immediately after as well as 2 min, 5 min, and 30 min after the tap.

Targeted Illumination

All targeted illuminations were performed with Leica model DMI600 and Mosaic 2 (Andor Technologies). For behavior experiments, low-intensity halogen light was used to visualize the worm, whereas the Mosaic micromirror array targeted individual neurons with blue light (450–480 nm) from an LED light source (XLED, Lumen Dynamics). For GCaMP3 measurements, the whole field of view was illuminated with blue light (450–480 nm) from the XLED, which was further attenuated with an external 435–470 nm optical filter, whereas the Mosaic micromirror array targeted individual neurons with higher-intensity blue light (450–480 nm).

Modeling

All simulations were performed using custom scripts in Matlab with parameters and equations previously published (Kashtan et al., 2004). Individual variables (e.g., ASH activity) were generated by allowing the script to generate values at the various input values where other variables (ASH threshold, AVD threshold, AVA threshold) were fixed. The script ran variations of different combinations to generate the data plotted in the activity versus time plots shown in Figure S7B.

SUPPLEMENTAL INFORMATION

Supplemental Information includes six figures and two movies and can be found with this article online at http://dx.doi.org/10.1016/j.cell.2013.11.036.

ACKNOWLEDGMENTS

We thank William Schafer (University of Cambridge), Alexander Gottschalk (Johann Wolfgang Goethe University), Elissa Hallem (University of California, Los Angeles), and the Caenorhabditis Genetics Center (University of Minnesota) for worm strains and Karl Deisseroth (Stanford University) for channelrhodopsin constructs. We also thank David Anderson, David Prober, Alon Zaslaver, Trevor Fowler, and Lauren Lebon for their input and Meenakshi Doma, Yen-ping Hsueh, Mihoko Kato, Hillel Schwartz, and members of our lab for editorial comments. J.Y.C. was supported by National Institutes of Health USPHS training grant GM07616. This work was supported by the Howard Hughes Medical Institute, with which P.W.S. is an investigator, and by NIH grant DA018341 to P.W.S.

Received: May 25, 2013
Revised: September 26, 2013
Accepted: November 15, 2013
Published: January 16, 2014

REFERENCES

Allada, R., and Siegel, J.M. (2008). Unearthing the phylogenetic roots of sleep. Curr. Biol. *18*, R670–R679.

Bargmann, C.I. (2006). Chemosensation in C. elegans. WormBook, 1–29.

Ben Arous, J., Tanizawa, Y., Rabinowitch, I., Chatenay, D., and Schafer, W.R. (2010). Automated imaging of neuronal activity in freely behaving Caenorhabditis elegans. J. Neurosci. Methods *187*, 229–234.

Brenner, S. (1974). The genetics of *Caenorhabditis elegans*. Genetics *77*, 71–94.

Chalfie, M., Sulston, J.E., White, J.G., Southgate, E., Thomson, J.N., and Brenner, S. (1985). The neural circuit for touch sensitivity in Caenorhabditis elegans. J. Neurosci. *5*, 956–964.

Chatzigeorgiou, M., and Schafer, W.R. (2011). Lateral facilitation between primary mechanosensory neurons controls nose touch perception in C. elegans. Neuron *70*, 299–309.

Chronis, N., Zimmer, M., and Bargmann, C.I. (2007). Microfluidics for in vivo imaging of neuronal and behavioral activity in Caenorhabditis elegans. Nat. Methods *4*, 727–731.

Dabbish, N.S., and Raizen, D.M. (2011). GABAergic synaptic plasticity during a developmentally regulated sleep-like state in C. elegans. J. Neurosci. *31*, 15932–15943.

Ezcurra, M., Tanizawa, Y., Swoboda, P., and Schafer, W.R. (2011). Food sensitizes C. elegans avoidance behaviours through acute dopamine signalling. EMBO J. *30*, 1110–1122.

Foltenyi, K., Greenspan, R.J., and Newport, J.W. (2007). Activation of EGFR and ERK by rhomboid signaling regulates the consolidation and maintenance of sleep in Drosophila. Nat. Neurosci. *10*, 1160–1167.

Guo, Z.V., Hart, A.C., and Ramanathan, S. (2009). Optical interrogation of neural circuits in Caenorhabditis elegans. Nat. Methods *6*, 891–896.

Hilliard, M.A., Bargmann, C.I., and Bazzicalupo, P. (2002). C. elegans responds to chemical repellents by integrating sensory inputs from the head and the tail. Curr. Biol. *12*, 730–734.

Hilliard, M.A., Apicella, A.J., Kerr, R., Suzuki, H., Bazzicalupo, P., and Schafer, W.R. (2005). In vivo imaging of C. elegans ASH neurons: cellular response and adaptation to chemical repellents. EMBO J. *24*, 63–72.

Jones, E.G. (2009). Synchrony in the interconnected circuitry of the thalamus and cerebral cortex. Ann. N Y Acad. Sci. *1157*, 10–23.

Kashtan, N., Itzkovitz, S., Milo, R., and Alon, U. (2004). Topological generalizations of network motifs. Phys. Rev. E Stat. Nonlin. Soft Matter Phys. *70*, 031909.

Letzkus, J.J., Wolff, S.B., Meyer, E.M., Tovote, P., Courtin, J., Herry, C., and Lüthi, A. (2011). A disinhibitory microcircuit for associative fear learning in the auditory cortex. Nature *480*, 331–335.

Li, W., Kang, L., Piggott, B.J., Feng, Z., and Xu, X.Z. (2011). The neural circuits and sensory channels mediating harsh touch sensation in Caenorhabditis elegans. Nat Commun *2*, 315.

Lindsay, T.H., Thiele, T.R., and Lockery, S.R. (2011). Optogenetic analysis of synaptic transmission in the central nervous system of the nematode Caenorhabditis elegans. Nat Commun *2*, 306.

Magnin, M., Rey, M., Bastuji, H., Guillemant, P., Mauguière, F., and Garcia-Larrea, L. (2010). Thalamic deactivation at sleep onset precedes that of the cerebral cortex in humans. Proc. Natl. Acad. Sci. USA *107*, 3829–3833.

Metherate, R. (2004). Nicotinic acetylcholine receptors in sensory cortex. Learn. Mem. *11*, 50–59.

Metherate, R., and Hsieh, C.Y. (2004). Synaptic mechanisms and cholinergic regulation in auditory cortex. Prog. Brain Res. *145*, 143–156.

Monsalve, G.C., Van Buskirk, C., and Frand, A.R. (2011). LIN-42/PERIOD controls cyclical and developmental progression of *C. elegans* molts. Curr. Biol. *21*, 2033–2045.

Narayan, A., Laurent, G., and Sternberg, P.W. (2011). Transfer characteristics of a thermosensory synapse in Caenorhabditis elegans. Proc. Natl. Acad. Sci. USA *108*, 9667–9672.

Park, J.W., Vahidi, B., Taylor, A.M., Rhee, S.W., and Jeon, N.L. (2006). Microfluidic culture platform for neuroscience research. Nat. Protoc. *1*, 2128–2136.

Raizen, D.M., Zimmerman, J.E., Maycock, M.H., Ta, U.D., You, Y.J., Sundaram, M.V., and Pack, A.I. (2008). Lethargus is a Caenorhabditis elegans sleep-like state. Nature *451*, 569–572.

Schmitt, C., Schultheis, C., Pokala, N., Husson, S.J., Liewald, J.F., Bargmann, C.I., and Gottschalk, A. (2012). Specific expression of channelrhodopsin-2 in single neurons of Caenorhabditis elegans. PLoS ONE *7*, e43164.

Schwarz, J., Lewandrowski, I., and Bringmann, H. (2011). Reduced activity of a sensory neuron during a sleep-like state in Caenorhabditis elegans. Curr. Biol. *21*, R983–R984.

Siegel, J.M. (2001). The REM sleep-memory consolidation hypothesis. Science *294*, 1058–1063.

Van Buskirk, C., and Sternberg, P.W. (2007). Epidermal growth factor signaling induces behavioral quiescence in Caenorhabditis elegans. Nat. Neurosci. *10*, 1300–1307.

Ward, S., Thomson, N., White, J.G., and Brenner, S. (1975). Electron microscopical reconstruction of the anterior sensory anatomy of the nematode Caenorhabditis elegans.?2UU. J. Comp. Neurol. *160*, 313–337.

White, J.G., Southgate, E., Thomson, J.N., and Brenner, S. (1986). The structure of the nervous system of the nematode Caenorhabditis elegans. Philos. Trans. R. Soc. Lond. B Biol. Sci. *314*, 1–340.

Yizhar, O., Fenno, L.E., Davidson, T.J., Mogri, M., and Deisseroth, K. (2011). Optogenetics in neural systems. Neuron *71*, 9–34.

You, Y.J., Kim, J., Raizen, D.M., and Avery, L. (2008). Insulin, cGMP, and TGF-beta signals regulate food intake and quiescence in C. elegans: a model for satiety. Cell Metab. *7*, 249–257.

Zhang, F., Wang, L.P., Brauner, M., Liewald, J.F., Kay, K., Watzke, N., Wood, P.G., Bamberg, E., Nagel, G., Gottschalk, A., and Deisseroth, K. (2007). Multimodal fast optical interrogation of neural circuitry. Nature *446*, 633–639.

Zimmerman, J.E., Naidoo, N., Raizen, D.M., and Pack, A.I. (2008). Conservation of sleep: insights from non-mammalian model systems. Trends Neurosci. *31*, 371–376.